

## Simplified LCAO Method for Zincblende, Wurtzite, and Mixed Crystal Structures\*

JOSEPH L. BIRMAN

*Research Laboratories, Sylvania Electric Products Incorporated, Bayside, New York*

(Received January 22, 1959)

The tight-binding (LCAO) method is a convenient, if qualitative, way of comparing energy bands in the zincblende and wurtzite structures. Using this method it is shown that wurtzite states along  $\Gamma-\Gamma'$  ("c" direction in the zone) can be obtained by perturbing corresponding zincblende states along  $\Gamma-\Lambda$  ([111] zone direction). The perturbation is the difference of crystal potential,  $V' = V(\text{ZB}) - V(\text{Wur})$ , which takes the zincblende structure into the wurtzite and results in a splitting and shifting of these corresponding states. For  $\mathbf{k}$  perpendicular to these directions the correspondence of  $\mathbf{k}$  vectors and of states is not so clear, although some comparison can still be made.

The discussion of corresponding zincblende and wurtzite states is helpful in understanding the nature of the energy states in mixed crystals: (wurtzite structure [111] twinned on zincblende), and in faulted crystals: [111] stacking faults. We can show that barriers (discontinuities in energy surfaces) exist for electron propagation (current) parallel to the "c" axis of a twinned or faulted crystal due to two effects: a symmetry effect and a polar effect. The second effect is simply illustrated for rotation-twinned zincblende. For randomly faulted crystals, band gaps depend on  $\alpha$ , the probability of faulting. Quantitative theories of these effects remain to be developed.

## 1. INTRODUCTION

THE discussion to be presented in this paper is an outgrowth of work specifically connected with the cellular calculation of the band structure of ZnS in zincblende (ZB) and wurtzite (Wur) structures. Although the writer's primary interest is in the band structure of ZnS, the "simplified LCAO method" to be discussed here can equally well be applied to other materials which are dimorphic with zincblende and wurtzite structures and which have valence and conduction bands "s"- and "p"-like, for example SiC, CdS, CdSe, etc.<sup>1</sup> While this method does allow certain general conclusions to be drawn about band structures in the two crystalline forms it must be emphasized that only specific knowledge for each material is reliable, and hence no general statements can replace detailed calculations and experiment for each particular compound. On the other hand, the general conclusions one can draw in the LCAO (linear combination of atomic orbitals) framework are free of the particular assumptions needed for detailed cellular<sup>2</sup> or OPW (orthogonalized plane waves), or PW (plane waves), or variational type calculations, such as sphericity of potential, or number of terms kept in Fourier expansions, etc., and therefore may be helpful as a framework. The LCAO method<sup>3</sup> has an additional advantage for this discussion, namely that its formalism enables one to make direct

use of the similarity of first and second neighbor arrangements in zincblende and wurtzite. Not only can we compare the (structurally) pure zincblende and wurtzite energy states, but also we shall examine the effect on the band structure of a particular stacking fault (the rotation twin in zincblende), and of the existence of [111] twin crystals (zincblende regions twinned on wurtzite). Again, although particularly aimed at ZnS, the discussion will apply as well to other dimorphic materials.<sup>4</sup>

## 2. COORDINATE SYSTEMS: SYMMETRY ELEMENTS IN CRYSTAL SPACE

It is usually convenient<sup>5</sup> to describe atomic positions in zincblende (space group  $T_d^2$ ) in terms of a Cartesian set of axes coinciding with the cubic  $x, y, z$  axes; in wurtzite (space group  $C_{6v}^4$ ) hexagonal axes are introduced in a similarly conventional manner. The unit cells on these axes are shown in Fig. 1. However, use of these different axis systems in each structure obscures similarities long since known to crystallographers.<sup>6</sup> Hence, we define a new set of Cartesian axes in zincblende:

$$\begin{pmatrix} i' \\ j' \\ k' \end{pmatrix} = \begin{pmatrix} 0 & 1/\sqrt{2} & -1/\sqrt{2} \\ -2/\sqrt{6} & 1/\sqrt{6} & 1/\sqrt{6} \\ 1/\sqrt{3} & 1/\sqrt{3} & 1/\sqrt{3} \end{pmatrix} \begin{pmatrix} i \\ j \\ k \end{pmatrix}, \quad (1)$$

where  $\mathbf{i}, \mathbf{j}, \mathbf{k}$  are the old Cartesian set. With this choice of directions  $\mathbf{k}'$  or  $\mathbf{z}'$  in zincblende is along the cube body diagonal ([111] direction) or three fold rotation axis 3, and the  $y$  axis is on a mirror plane  $\sigma_d$ . This is shown in Fig. 2. The same Cartesian axes will be used in wurtzite, and Fig. 2 also shows their orientation with respect to the conventional hexagonal axes  $\mathbf{a}_1, \mathbf{a}_2$ . The

\* Most of the material of this paper was presented at the American Physical Society Meeting, March, 1958, Chicago, Illinois [Bull. Am. Phys. Soc. II, 3, 121 (1958)].

<sup>1</sup> Although the entire discussion in this paper is (except where noted) of general applicability to all compounds with zincblende and wurtzite structures, where it is necessary to make an illustration, we shall refer to ZnS specifically, as a typical compound (this is particularly true in the figures).

<sup>2</sup> J. Birman, Phys. Rev. **109**, 810 (1958); C. Shakin and J. Birman, Phys. Rev. **109**, 818 (1958). See also F. Hund and B. Mrowka, Ber. Säch. Akad. (Math. Phys. Klasse) **87**, 185, 325 (1935) for an earlier treatment of the zincblende-wurtzite problem by a cellular type method.

<sup>3</sup> J. Slater and G. Koster, Phys. Rev. **94**, 1498 (1954).

<sup>4</sup> Jeffrey, Parry, and Mozzi, J. Chem. Phys. **25**, 1024 (1956), Table I.

<sup>5</sup> W. Zachariasen, *Theory of X-ray Diffraction in Crystals* (John Wiley & Sons, Inc., New York, 1945), Table 2.6, p. 51.

<sup>6</sup> G. Aminoff and A. Broomé, Z. Krist. **80**, 355 (1931).

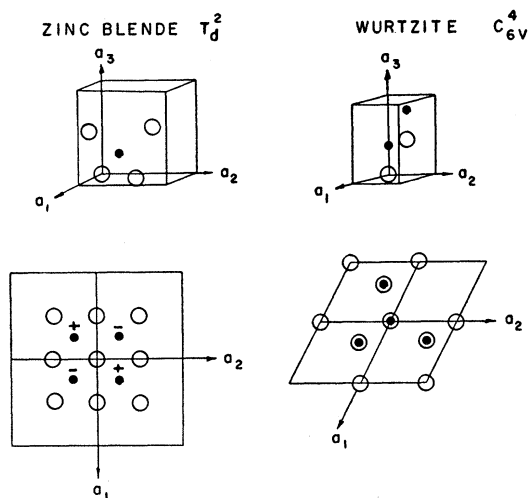


FIG. 1. Unit cells of zincblende and wurtzite on conventional Cartesian or hexagonal axes. (Sulfur atom is at the origin.) Base plane ( $z=0$ ) projection is shown in the lower half of the figure. In this, and the following figures sulfur atom is shown as the larger, open circle, zinc as the smaller blackened circle [see footnote (1)].

$x'y'$  plane contains three different types of sites, labeled  $A, B, C$ , in Fig. 2; only one of these types is occupied in any given plane, giving rise to a close packed net (i.e., a net such that the nuclei are in the close packed position—no implication as to atom/ion sizes is meant). In both structures Zn and S close packed nets alternate, and in both after one Zn-S double layer another follows, in a displaced position. This is illustrated in Fig. 3 in terms of a "stacking diagram" or  $[110]$  section through zincblende and wurtzite.

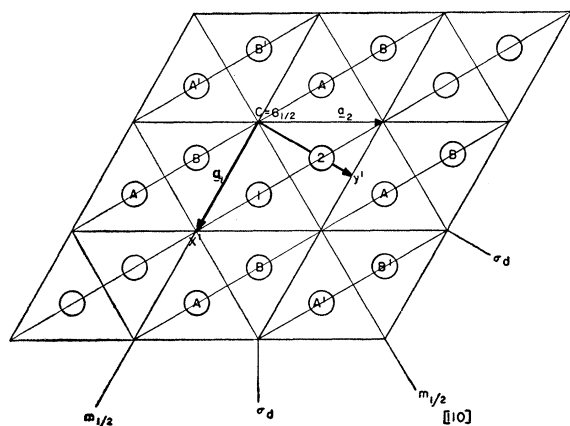


FIG. 2. Base plane projection of the wurtzite structure (only sulfur atoms are shown); conventional hexagonal axes are shown as  $a_1, a_2$ . Sites  $A, B, C$  are indicated; the origin is at  $C$ , along the six fold screw axis. The  $x'$  direction is along  $a_1$  (the glide plane,  $m_3$ , contains  $x'$ ) the  $y'$  direction along the mirror plane,  $\sigma_d$ . The magnitude of vector  $x'=\alpha$ , that of vector  $y'=\beta$  [see Eq. (2)]. The twelve second neighbors of sulfur atom (1) are the six labeled  $A$ , in the plane, and three  $B$  above and three below the plane. In zincblende the sites  $C$  are occupied by S (and Zn) atoms, hence the axis along  $c$  is no longer  $6_3$ , and the  $x'$  no longer on a  $m_3$ . The  $(11\cdot0)$  planes are perpendicular to the  $[11\cdot0]$  direction indicated.

In Table I the coordinates of the atoms of the base are given with a variety of choices of origin, in terms of the conventional zincblende and wurtzite axis systems. If  $a$  is the distance between neighbors in the close packed plane (Fig. 2) it is convenient to measure distances along  $(x', y', z')$  in units of  $(\alpha, \beta, \gamma)$ , respectively, where<sup>7</sup>

$$\alpha = a/2, \quad \beta = \sqrt{3}a/2, \quad \gamma = \frac{1}{2}(\frac{3}{8})^{1/2}a = c/2. \quad (2)$$

In Table II first and second neighbors of the S atom at the origin in zincblende, and of the two S atoms of the base in wurtzite, are given in conventional units and in units of  $(\alpha, \beta, \gamma)$ . The identity of first neighbor shells, and the close similarity of second neighbor shells in the two structures, can be obtained from the coordinates in Table II. In Fig. 4 a perspective drawing of the first and second neighbor arrangements in zincblende and wurtzite is shown.

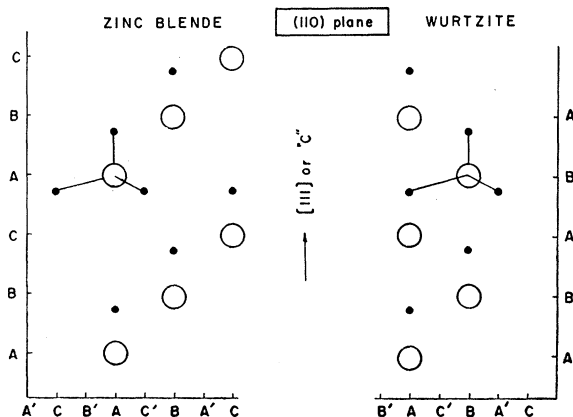


FIG. 3. Stacking diagram or  $[11\cdot0]$  section through zincblende and wurtzite. Note the 3 layer zincblende repeat, and the 2 layer wurtzite repeat. The primed sites ( $A'$ , etc.) are on  $(11\cdot0)$  planes displaced from the origin (see Fig. 2). Hence 2 of the 4 Zn neighbors are on the same  $(11\cdot0)$  plane as the S atom indicated, while the other 2 are one each in front and behind the plane of the drawing.

It will later be convenient for us to have available symmetry elements for the space groups  $T_d^2$  and  $C_{6v}^4$ . These are given in Table III, with the operations expressed in terms of the primed Cartesian coordinate system (1) illustrated in Fig. 2. We shall choose our origin of coordinates in zincblende at the site  $C$ , which is occupied by an S atom, and at the same point in wurtzite, which is on the six-fold screw axis, (not occupied by any atom). It is of interest to note that the site symmetry in zincblende is  $T_d = \bar{4}3m$ , while in wurtzite it is only  $C_{3v} = 3m$ ; that is, although in the ideal wurtzite structure each S is tetrahedrally surrounded by 4 first neighbor Zn, the four are not equivalent. The symmetry elements given in Table III are needed in formally reducing the  $E$  integrals which arise in the LCAO<sup>8</sup> method and in specifying  $G(\mathbf{k})$ , the group

<sup>7</sup> M. Miasek, Phys. Rev. **107**, 92 (1957).

TABLE I. Coordinates of the base atoms in zincblende (ZB) and wurtzite (Wur). Column (a): coordinates in terms of the usual Cartesian axes [see J. Birman, Phys. Rev. **109**, 810 (1958), Table I]; (b), (d), (f), (h): Coordinates in primed Cartesian axes ( $\alpha, \beta, \gamma$ ) [see text Eqs. (1) and (2)]. We have used  $u=3/8$  here; (c), (e), (g): Coordinates in conventional hexagonal axes. Note atoms labelled  $\textcircled{1}$   $\textcircled{2}$   $\textcircled{3}$   $\textcircled{4}$  and see Figs. 2 and 3. Columns (a) and (b) are for ZB, Columns (c), (d), (e), (f), (g), (h) for Wur.

Structure Origin at	ZB A, B, or C		Wur <sup>a</sup>					
	(a)	(b)	(c)	(d)	(e)	(f)	(g)	(h)
S $\textcircled{1}$	(0, 0, 0)	(0, 0, 0)	(0, 0, 0)	(0, 0, 0)	(0, 0, 0)	(0, 0, 0)	(1/3, 2/3, 0)	(0, 2/3, 0)
S $\textcircled{2}$			(2/3, 1/3, 1/2)	(1, 1/3, 1)	(1/3, 2/3, 1/2)	(0, 2/3, 1)	(2/3, 1/3, 1/2)	(1, 1/3, 1)
Zn $\textcircled{3}$	(1/2, 1/2, 1/2)	(0, 0, 3/4)	(0, 0, $u$ )	(0, 0, 3/4)	(0, 0, $u$ )	(0, 0, 3/4)	(1/3, 2/3, $u$ )	(0, 2/3, 3/4)
Zn $\textcircled{4}$			(2/3, 1/3, $u+1/2$ )	(1, 1/3, 7/4)	(1/3, 2/3, $u+1/2$ )	(0, 2/3, 7/4)	(2/3, 1/3, $u+1/2$ )	(1, 1/3, 7/4)

<sup>a</sup>  $u=3/8$  in the "ideal" wurtzite structure.

of the wave vector at various points of interest in the Brillouin zones.

### 3. ZONES AND CORRESPONDING $k$ VECTORS

To facilitate the comparison between zincblende and wurtzite zones and  $\mathbf{k}$  vectors, it is now necessary to take into account the difference in base (2 atoms in zincblende, 4 in wurtzite): Table I. We introduce the Jones or energy zone<sup>8</sup> for the two structures and suppose that we deal with a zincblende crystal, and a wurtzite crystal (grundgebiet)<sup>9</sup> each containing the same number of atoms, and hence half as many primitive cells in wurtzite as in zincblende. The Jones zone of wurtzite is twice the volume of the reduced zone of wurtzite, while the Jones zone of zincblende is identical with the reduced zone (the familiar truncated octahedron). Both Jones zones contain the same number of

states per atom. These zones are shown in Fig. 5. A number of points of interest in the two zones are marked. The median section ( $k_x'k_y'$  plane) through the zones is shown in Fig. 6. In Table IV the coordinates of various points in both zones are given in terms of<sup>7</sup>

$$\xi = \alpha k_{x'}, \quad \eta = \beta k_{y'}, \quad \zeta = \gamma k_{z'}, \quad (3)$$

where  $k_{x'}$ ,  $k_{y'}$ ,  $k_{z'}$  are the Cartesian components of the  $\mathbf{k}$  vector, parallel to the primed system (1), and ( $\alpha, \beta, \gamma$ ) have been defined in (2). We now discuss  $\mathbf{k}$  vectors along the polar ("c" or  $[111]$ ) directions:  $\Gamma-\Lambda$ (ZB) and  $\Gamma-\Gamma'$ (Wur) and perpendicular to them:  $\Gamma-K$  and  $\Gamma-M$  in both structures.

Now, to each  $\mathbf{k}$  along  $\Gamma-\Lambda$ (ZB), there corresponds an *identical*  $\mathbf{k}$  along  $\Gamma-\Gamma'$ (Wur), from  $\mathbf{k}=\Gamma$  to  $\mathbf{k}=\Lambda$  or  $\Gamma'$ . Thus, considering plane wave propagation, we may choose plane waves of exactly corresponding wave

TABLE II. First and second neighbors of the base atoms, zincblende (ZB) and wurtzite (Wur). Column (a): coordinates in terms of the usual Cartesian axes; (b), (d), (f): Coordinates in terms of ( $\alpha, \beta, \gamma$ ) [see Text Eq. (1) and (2)]; (c), (e): Coordinates in conventional hexagonal axes. Columns (a) and (b) are for ZB, columns (c), (d), (e), (f) for Wur.

Structure Base atom	ZB <sup>a</sup>		Wur <sup>b</sup>			
	(a)	(b)	(c)	(d)	(e)	(f)
			(2/3, 1/3, 1/2) = (1, 1/3, 1)		(1/3, 2/3, 0) = (0, 2/3, 0)	
			First Neighbors			
	(1/2, 1/2, 1/2)	(0, 0, 3/4)	(2/3, 1/3, 7/8)	(1, 1/3, 7/4)	(1/3, 2/3, 3/8)	(0, 2/3, 3/4)
	(1/2, -1/2, -1/2)	(0, -2/3, -1/4)	(1/3, -1/3, 3/8)	(1, -1/3, 3/4)	(2/3, 4/3, -1/8)	(0, 4/3, -1/4)
	(-1/2, -1/2, 1/2)	(-1, 1/3, -1/4)	(1/3, 2/3, 3/8)	(0, 2/3, 3/4)	(-1/3, 1/3, -1/8)	(-1, 1/3, -1/4)
	(-1/2, 1/2, -1/2)	(1, 1/3, -1/4)	(4/3, 2/3, 3/8)	(2, 2/3, 3/4)	(2/3, 1/3, -1/8)	(1, 1/3, -1/4)
			Second Neighbors			
	(1, 1, 0)	(1, -1/3, 1)	(4/3, 2/3, 1)	(2, 2/3, 2)	(-1/3, 1/3, -1/2)	(-1, 1/3, -1)
	(1, -1, 0)	(-1, -1, 0)	(-1/3, -2/3, 1/2)	(0, -2/3, 1)	(-2/3, -1/3, 0)	(-1, -1/3, 0)
	(-1, 1, 0)	(1, 1, 0)	(5/3, 4/3, 1)	(2, 4/3, 1)	(-1/3, 1/3, +1/2)	(-1, 1/3, 1)
	(-1, -1, 0)	(-1, 1/3, -1)	(1/3, 2/3, 0)	(0, 2/3, 0)	(1/3, -1/3, 0)	(1, -1/3, 0)
	(1, 0, 1)	(-1, -1/3, 1)	(1/3, -1/3, 1)	(1, -1/3, 2)	(2/3, 1/3, -1/2)	(1, 1/3, -1)
	(1, 0, -1)	(1, -1, 0)	(2/3, -2/3, 1/2)	(2, -2/3, 1)	(2/3, 1/3, +1/2)	(1, 1/3, 1)
	(-1, 0, 1)	(-1, 1, 0)	(2/3, 4/3, 1/2)	(0, 4/3, 1)	(2/3, 4/3, -1/2)	(0, 4/3, -1)
	(-1, 0, -1)	(1, 1/3, -1)	(4/3, 2/3, 0)	(2, 2/3, 0)	(4/3, 2/3, 0)	(2, 2/3, 0)
	(0, 1, 1)	(0, 2/3, 1)	(1/3, 2/3, 1)	(0, 2/3, 2)	(2/3, 4/3, +1/2)	(0, 4/3, 1)
	(0, 1, -1)	(2, 0, 0)	(5/3, 1/3, 1/2)	(3, 1/3, 1)	(4/3, 5/3, 0)	(1, 5/3, 0)
	(0, -1, 1)	(-2, 0, 0)	(-1/3, 1/3, 1/2)	(-1, 1/3, 1)	(-2/3, 2/3, 0)	(-2, 2/3, 0)
	(0, -1, -1)	(0, -2/3, 1)	(1/3, -1/3, 0)	(1, -1/3, 0)	(1/3, 5/3, 0)	(-1, 5/3, 0)

<sup>a</sup> Origin at a sulfur site.

<sup>b</sup> Origin at site C (see Table I).

<sup>8</sup> J. R. Reitz, *Solid State Physics* (Academic Press, New York, 1955), Vol. 1, p. 32; A. H. Wilson, *Theory of Metals* (Cambridge University Press, Cambridge, 1953), second edition, p. 90.

<sup>9</sup> J. C. Slater, *Handbuch der Physik* (Springer-Verlag, Berlin, 1956), Vol. 19, p. 13; A. Sommerfeld and H. Bethe, *Handbuch der Physik* (Verlag Julius Springer, Berlin, 1933), Vol. 24, part 2, p. 373.

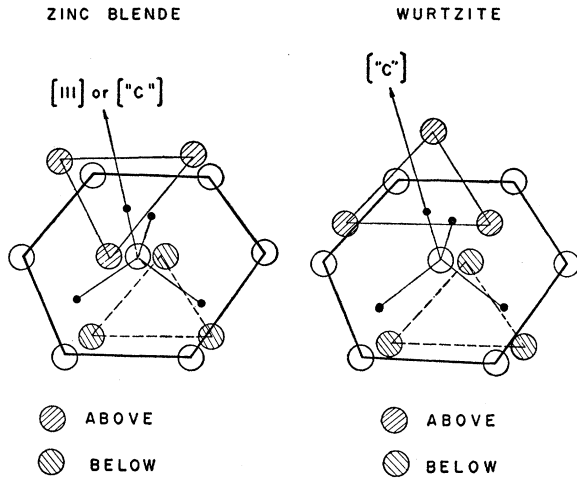


FIG. 4. First and second neighbors in zincblende and wurtzite. Large circles are S atoms, small ones Zn. Open circles are in the same plane. Comparing the two structures, we note that only three of the twelve second neighbors differ, and even these are disposed symmetrically. These are shown as the 3 atoms "above" and are rotated by  $\pi/3$  in comparing zincblende and wurtzite.

lengths in both structures. The planes of constant phase (close packed nets) are, of course, the same in both structures, alternating Zn and S as discussed above. The minimum wavelength ( $k = k_{\max}$ ) is  $\lambda = 2d_{111}$  where  $d_{111}$  is the Zn-Zn or S-S interplanar spacing. This is illustrated in Fig. 7.

The situation along  $\Gamma-K$  and  $\Gamma-M$  is not so

clear. As shown in Fig. 6, the distance  $\Gamma-K(\text{ZB}) > \Gamma-K(\text{Wur})$ . In fact, as Herring has shown<sup>10</sup> a wave vector along the prolongation of  $\Gamma-K(\text{Wur})$ , is equivalent (differs by a lattice vector in the Fourier Space) to a vector along the line  $K'-M'$ . The point in the wurtzite zone equivalent to  $K(\text{ZB})$  is shown as "encircled  $K$ " in Fig. 6. In words this means that we cannot propagate a single plane wave (chosen from within or on the energy zone) in wurtzite in the direction  $\Gamma-K$  with wavelength equal to the wavelength of the vector  $K(\text{ZB})$ , but we must superimpose 2 plane waves: "encircled  $K$ " plus  $(-b_1 + b_2)$ . Similarly  $M(\text{Wur})$  does not coincide with  $M(\text{ZB})$ ; the point equivalent to  $M(\text{ZB})$  is shown as "encircled  $M$ " in Fig. 6. This lack of identity of zincblende and wurtzite points  $K$  and  $M$  makes for ambiguity in the comparison of states along  $\Gamma-K$  and  $\Gamma-M$ . We may either (a) compare states at the same  $k$  thus necessitating folding of certain wurtzite  $k$  vectors as discussed above, or (b) compare states at the same fraction of  $k_{\max}$  along these directions. A third alternative, possible since the two energy zones contain the same number of states, would be to shift all zincblende  $k$ 's which are outside the corresponding wurtzite volume in such a way as to duplicate this volume, and then to identify wurtzite states and shifted zincblende states. In Fig. 8 we illustrate the plane wave propagation at points  $K$  and  $M$  in zincblende and wurtzite, showing the shortest waves which may occur in these directions.

While  $\Gamma-X$  is a principal symmetry direction in zinc-

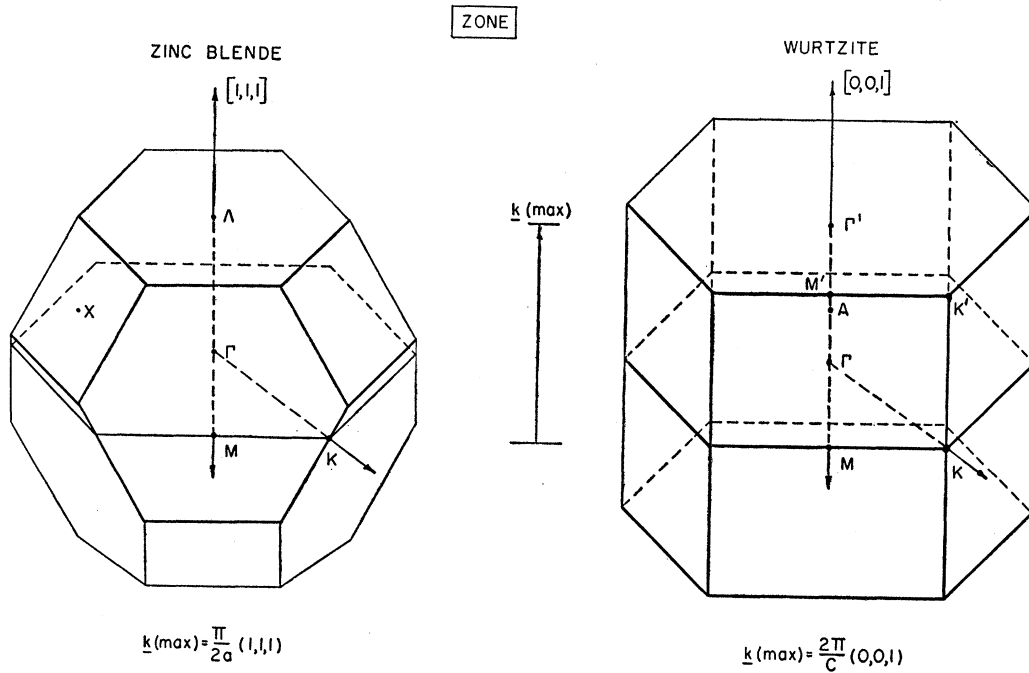


FIG. 5. Jones zones for zincblende and wurtzite. Each zone has volume  $= \pi^3 \sqrt{2} / \alpha^3$ .  $\alpha$  is defined in Eq. (2). Now  $|\Gamma-\Lambda| = |\Gamma-\Gamma'| = |\underline{k}_{\max}|$ . For the section perpendicular to  $c$  see Fig. 6.

<sup>10</sup> C. Herring, J. Franklin Inst. 233, 525 (1942).

blende, it is clear from Fig. 5 that no principal direction in the wurtzite zone corresponds to it. Consequently we shall not attempt to make a correspondence for  $\mathbf{k}$  vectors, or states, along this direction, even though the zincblende secular determinant factors simply (see reference 3, p. 1522).

#### 4. CRYSTAL POTENTIAL IN ZINCBLLENDE AND WURTZITE

In discussing the relationship between the crystal potential in zincblende:  $V(\text{ZB})$ , and in wurtzite:

TABLE III. Symmetry elements zincblende and wurtzite.<sup>a,b</sup>

	Zincblende			
3:	$\begin{pmatrix} -1/2 & -\sqrt{3}/2 & 0 \\ \sqrt{3}/2 & -1/2 & 0 \\ 0 & 0 & 1 \end{pmatrix}$			
$m \cdots (yz)$ :	$\begin{pmatrix} -1 & 0 & 0 \\ 0 & 1 & 0 \\ 0 & 0 & 1 \end{pmatrix}$			
2:	$\begin{pmatrix} -1 & 0 & 0 \\ 0 & 1/3 & -4/3\sqrt{2} \\ 0 & -4/3\sqrt{2} & -1/3 \end{pmatrix}$			
$\bar{4}$ :	$\begin{pmatrix} 0 & -1/\sqrt{3} & -2/\sqrt{6} \\ 1/\sqrt{3} & -2/3 & 2/3\sqrt{2} \\ 2/\sqrt{6} & 2/3\sqrt{2} & -1/3 \end{pmatrix}$			
$m'$ :	$\begin{pmatrix} 1/2 & +1/(12)^{\dagger} & -2/\sqrt{6} \\ +1/(12)^{\dagger} & 5/6 & 2/(18)^{\dagger} \\ -2/\sqrt{6} & 2/(18)^{\dagger} & -1/3 \end{pmatrix}$	$\begin{pmatrix} 0 & 0 & -1 \\ 0 & 1 & 0 \\ -1 & 0 & 0 \end{pmatrix}^{\circ}$		
$m''$ :	$\begin{pmatrix} 1/2 & 3/(12)^{\dagger} & 0 \\ 3/(12)^{\dagger} & -1/2 & 0 \\ 0 & 0 & 1 \end{pmatrix}$	$\begin{pmatrix} 0 & 0 & 1 \\ 0 & 1 & 0 \\ 1 & 0 & 0 \end{pmatrix}^{\circ}$		
	Wurtzite			
$\sigma_z$ :	$\begin{pmatrix} 1/2 & -\sqrt{3}/2 & 0 \\ \sqrt{3}/2 & 1/2 & 0 \\ 0 & 0 & 1 \end{pmatrix}$	$\begin{pmatrix} 0 \\ 0 \\ a_3/2 \end{pmatrix}$		
$m_3(x)$ :	$\begin{pmatrix} 1 & 0 & 0 \\ 0 & -1 & 0 \\ 0 & 0 & 1 \end{pmatrix}$	$\begin{pmatrix} 0 \\ 0 \\ a_3/2 \end{pmatrix}$		
$m_3'(6x)$ :	$\begin{pmatrix} -1/2 & \sqrt{3}/2 & 0 \\ \sqrt{3}/2 & -1/2 & 0 \\ 0 & 0 & 1 \end{pmatrix}$	$\begin{pmatrix} 0 \\ 0 \\ a_3/2 \end{pmatrix}$		
$m_3''(6^2x)$ :	$\begin{pmatrix} -1/2 & -\sqrt{3}/2 & 0 \\ -\sqrt{3}/2 & 1/2 & 0 \\ 0 & 0 & 1 \end{pmatrix}$	$\begin{pmatrix} 0 \\ 0 \\ a_3/2 \end{pmatrix}$		
$\sigma_d(yz)$ :	$\begin{pmatrix} -1 & 0 & 0 \\ 0 & 1 & 0 \\ 0 & 0 & 1 \end{pmatrix}$			
$\sigma_d'(6^2yz)$ :	$\begin{pmatrix} 1/2 & \sqrt{3}/2 & 0 \\ \sqrt{3}/2 & -1/2 & 0 \\ 0 & 0 & 1 \end{pmatrix}$			

<sup>a</sup> These elements are convenient for later discussions rather than a generating set, in the sense of Zachariasen.<sup>5</sup>

<sup>b</sup> The elements are expressed in the primed Cartesian coordinate system, Eq. (1), except for those matrices indicated <sup>c</sup>: the latter are in terms of the original zincblende Cartesian system.

$V(\text{Wur})$ , one must distinguish two factors which enter: (a) the relationship between the bonding of a given compound in zincblende and *ideal* wurtzite structures, (b) the deviation of the wurtzite structure from ideality.

It is rather unlikely, on the face of it, that there be no difference in bonding when a compound occurs in

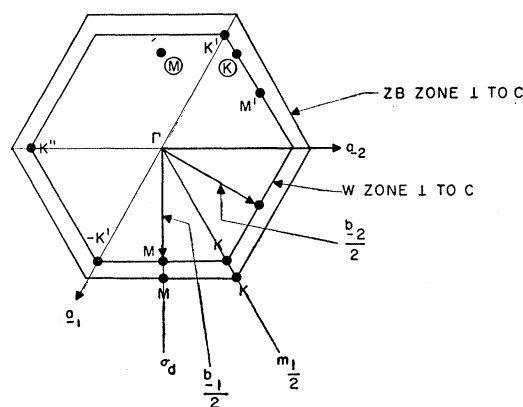


FIG. 6. Composite section through the zincblende and wurtzite Jones zones perpendicular to  $c$ . The outer hexagon refers to zincblende, the inner to wurtzite. The vectors  $\mathbf{b}_1/2$  and  $\mathbf{b}_2/2$  are half the wurtzite Fourier (reciprocal) lattice vectors, hence points  $K, K', K''$  in the wurtzite zone are equivalent. The point  $K(\text{ZB})$ , considered as a point in the wurtzite zone, is equivalent to "encircled  $K$ ," and similarly  $M(\text{ZB})$  and "encircled  $M$ " are equivalent. The point  $K'(\text{ZB})$ , [on the prolongation of  $\Gamma-K'(\text{Wur})$ ] is *not* equivalent to  $K(\text{ZB})$ .

either zincblende or wurtzite structures.<sup>11</sup> The nature of the bond may be characterized by specifying the crystal charge density  $\rho(\text{ZB})$  and  $\rho(\text{Wur})$  and these are amenable to experimental determination by refined x-ray Fourier synthesis techniques. To date no work has been reported on this important problem, although some recent x-ray work has gone on in dealing with certain zincblende and wurtzite structures separately.<sup>4,12</sup> From somewhat general arguments it seems likely that the chemical bond of the same compound in wurtzite structure should be more ionic than in zincblende structure.<sup>11</sup> For example, this may mean that the "effective charges" on the ions are somewhat greater in the wurtzite than in the zincblende structure.

Closely connected with this problem of bonding is that of the ideality of the wurtzite structure. We may take

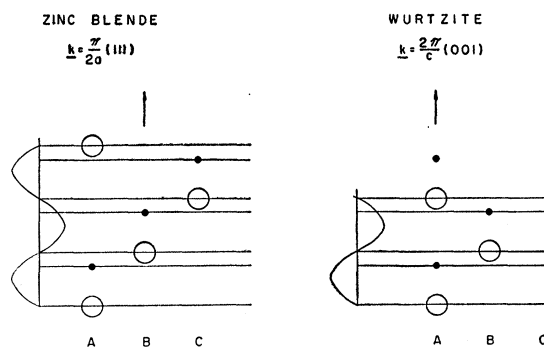


FIG. 7. Plane wave propagation at the edge of the zone in [ $c$ ] direction, at  $\mathbf{k}=\Lambda(\text{ZB})$  and  $\mathbf{k}=\Gamma'(\text{Wur})$ . Note that these shortest wavelength waves change phase by  $\pi$  on progressing from one close-packed plane to the next identical one, in either structure (i.e., from an S to an S plane).

<sup>11</sup> See A. v. Hippel, Z. Physik **133**, 158 (1952); reference 4; and also F. Keffer and A. M. Portis, J. Chem. Phys. **27**, 675 (1957).

<sup>12</sup> E. A. Jumpertz, Z. Elektrochem. **59**, 425 (1955).

TABLE IV. Coordinates of points in zincblende (ZB) and wurtzite (Wur) zones.

ZB	$\mathbf{k}$	$\mathbf{k} = (\xi, \eta, \zeta)$ See Eq. (3)	Wur	$\mathbf{k}$
$\Gamma$	(0, 0, 0)		$\Gamma$	(0, 0, 0)
$\Lambda$	(0, 0, $\pi$ )		$\Gamma'$	(0, 0, $\pi$ )
$K$	( $3\pi/8, 9\pi/8, 0$ )		$K$	( $\pi/3, \pi, 0$ )
$M$	( $9\pi/16, 9\pi/16, 0$ )		$M$	( $\pi/2, \pi/2, 0$ )

as prima facie evidence for the essential identity of bonding in zincblende and wurtzite structures the ideality of the latter. Our argument is if those forces tending to make the wurtzite structure locally ideal [ $u=3/8, c/a=(8/3)^{1/2}$ ] win out over other steric and ionic forces which tend to produce the nonideal wurtzite, then the bonding is essentially determined by first neighbor interaction. Now these first neighbor interactions may be essentially responsible for the existence of a stable zincblende structure, and consequently it seems reasonable to infer that if a compound exists in zincblende and (essentially) ideal wurtzite structures, the bonding is substantially the same in both. It would then be natural to use the same valence charge densities per atom pair:  $\rho(\text{ZB}) = \rho(\text{Wur}) = \rho_A + \rho_B$ , where  $A$  and  $B$  are the two atoms/ions (i.e., Zn and S) of the compound  $AB$ , in constructing the crystal potentials  $V(\text{ZB})$  and  $V(\text{Wur})$ . (This approach was used in the numerical work now under way for ZnS in zincblende and wurtzite structures.)<sup>2</sup>

If the same atom/ion charge densities are placed on both zincblende and ideal wurtzite lattices, then for the crystal potentials we may take

$$V(\text{ZB}) = V(\text{Wur}) + V', \quad (4)$$

where  $V'$  is a small perturbation. If the wurtzite structure differs from ideality ( $u \neq 3/8$ ), then  $V'$  will be the larger, as will the matrix elements computed from  $V'$ . In any event we shall use (4) in establishing various relationships between zincblende and wurtzite energy states.

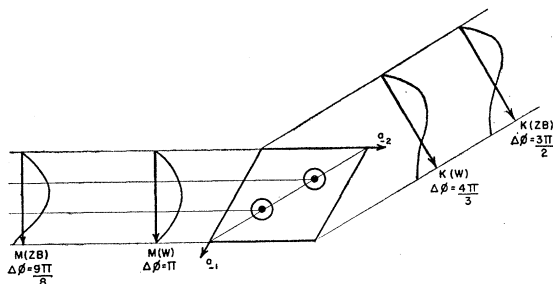


FIG. 8. Plane wave propagation at  $K$  and  $M$  in zincblende and wurtzite. Note the different phase changes  $\Delta\phi$  on progression through an identical distance (i.e., different wavelengths) making for ambiguity in comparison of states in zincblende and wurtzite along this direction. (See Text.)

## 5. CORRESPONDENCE BETWEEN STATES IN ZINCBLLENDE AND WURTZITE

In Table V we give, for various  $\mathbf{k}$  vectors of interest in zincblende<sup>13</sup> and, wurtzite<sup>14</sup>: (a) the symmetry ele-

TABLE V. LCAO Bloch functions<sup>a</sup> for zincblende and wurtzite.

Zincblende	
$\Gamma$ :	$G(\Gamma) = T_d = \bar{4}3m$
	$\Gamma_1 = as_1 + bs_3$
	$\textcircled{3}\Gamma'_4 = a(-2/(6)^{1/2}y_1 + 1/\sqrt{3}z_1) + b(-2/(6)^{1/2}y_3 + 1/\sqrt{3}z_3)$
$\Lambda$ :	$G(\Lambda) = C_{3v} = 3m$
	$\Lambda_1 = as_1 + bz_1 + cs_3 + dz_3$
	$\textcircled{2}\Lambda_3 = ax_1 + bx_3$
$K$ :	$G(K) = C_{1h} = m'$
	$K_{1e} = as_1 + b \left[ -\frac{x_1}{\sqrt{2}} + \frac{y_1}{(6)^{1/2}} + \frac{z_1}{\sqrt{3}} \right] + \frac{c}{\sqrt{2}} \left[ -\frac{x_1}{\sqrt{2}} - \frac{3}{(6)^{1/2}} y_1 \right]$
	$+ ds_3 + e \left[ -\frac{x_3}{\sqrt{2}} + \frac{y_3}{(6)^{1/2}} + \frac{z_3}{\sqrt{3}} \right] + \frac{f}{\sqrt{2}} \left[ -\frac{x_3}{\sqrt{2}} - \frac{3}{(6)^{1/2}} y_3 \right]$
	$K_{1o} = \frac{a}{\sqrt{2}} \left[ \frac{x_1}{\sqrt{2}} - \frac{y_1}{(6)^{1/2}} + \frac{2z_1}{\sqrt{3}} \right] + \frac{b}{\sqrt{2}} \left[ \frac{x_3}{\sqrt{2}} - \frac{y_3}{(6)^{1/2}} + \frac{2z_3}{\sqrt{3}} \right]$
$M$ :	$G(M) = C_{1h} = m''$
	$M_{1e} = as_1 + b \left[ \frac{x_1}{\sqrt{2}} + \frac{y_1}{(6)^{1/2}} + \frac{z_1}{\sqrt{3}} \right] + \frac{c}{\sqrt{2}} \left[ -\frac{x_1}{\sqrt{2}} - \frac{y_1}{(6)^{1/2}} + \frac{2z_1}{\sqrt{3}} \right]$
	$+ ds_3 + e \left[ \frac{x_3}{\sqrt{2}} + \frac{y_3}{(6)^{1/2}} + \frac{z_3}{\sqrt{3}} \right] + \frac{f}{\sqrt{2}} \left[ -\frac{x_3}{\sqrt{2}} - \frac{y_3}{(6)^{1/2}} + \frac{2z_3}{\sqrt{3}} \right]$
	$M_{1o} = a \left[ \frac{x_1}{2} - \frac{\sqrt{3}}{2} y_1 \right] + b \left[ \frac{x_3}{2} - \frac{\sqrt{3}}{2} y_3 \right]$
Wurtzite	
$\Gamma$ :	$G(\Gamma) = C_{6v} = 6_3m_3$
	$\Gamma_1 = (a/\sqrt{2})(s_1 + s_2) + (b/\sqrt{2})(z_1 + z_2)$
	$+ (c/\sqrt{2})(s_3 + s_4) + (d/\sqrt{2})(z_3 + z_4)$
	$\textcircled{2}\Gamma_5 = (a/\sqrt{2})(x_1 + x_2) + (b/\sqrt{2})(x_3 + x_4)$
$K$ :	$G(K) = C_{3v} = (6_3)^2m_3$
	$K_1 = (a/\sqrt{2})(s_1 + s_2) + (b/\sqrt{2})(z_1 + z_2)$
	$+ (c/\sqrt{2})(s_3 + s_4) + (d/\sqrt{2})(z_3 + z_4)$
	$\textcircled{2}K_3 = (a/\sqrt{2}) \{ (-\frac{1}{2}x_1 - (\sqrt{3}/2)y_1) + [ -\frac{1}{2}x_2 - (\sqrt{3}/2)y_2 ] \}$
	$+ (b/\sqrt{2}) \{ [ -\frac{1}{2}x_3 - (\sqrt{3}/2)y_3 ] + [ -\frac{1}{2}x_4 - (\sqrt{3}/2)y_4 ] \}$
$M$ :	$G(M) = C_{2v} = (6_3)^3\sigma_d' (6^3y_2)m_3'' (6^2x)$
	$M_1 = (a/\sqrt{2})(s_1 + s_2) + (b/\sqrt{2})(z_1 + z_2)$
	$+ (c/\sqrt{2})(s_3 + s_4) + (d/\sqrt{2})(z_3 + z_4)$
	$M_3 = a \left[ (x_1/2 - \sqrt{3}y_1/2) + (x_2/2 - \sqrt{3}y_2/2) \right]$
	$+ b \left[ (x_3/2 - \sqrt{3}y_3/2) + (x_4/2 - \sqrt{3}y_4/2) \right]$
	$M_4 = a \left[ (\sqrt{3}x_1/2 + y_1/2) + (\sqrt{3}x_2/2 + y_2/2) \right]$
	$+ b \left[ (\sqrt{3}x_3/2 + y_3/2) + (\sqrt{3}x_4/2 + y_4/2) \right]$

<sup>a</sup> All functions (Bloch sums) are expressed in terms of the primed axes Eq. (1). Where degeneracy exists the degree is indicated by a number in a circle, preceding the single partner which is given. For more conventional listing of the functions for ZB see D. Bell, Rev. Modern Phys. **26**, 311 (1954). The elements of various  $G(\mathbf{k})$  are explicitly given in Table III. In the functions,  $a, b, c, d, e$ , and  $f$  are constants.

<sup>13</sup> D. Bell, Revs. Modern Phys. **26**, 311 (1954); R. Parmenter, Phys. Rev. **100**, 573 (1955); G. Dresselhaus, Phys. Rev. **100**, 580 (1955).

<sup>14</sup> G. Dresselhaus, Phys. Rev. **105**, 135 (1957); W. J. O'Sullivan,

ments (see also Table III) contained in  $G(\mathbf{k})$ , the group of the wave vector  $\mathbf{k}$ , (b) the LCAO wave functions for the different states [irreducible representations of  $G(\mathbf{k})$ ] considered. A function such as  $x_j$  ( $j=1, 3$  for zinblende;  $j=1, 2, 3, 4$  for wurtzite; see Table I) is an orthonormalized Bloch sum of "x"-like Löwdin functions,<sup>3</sup> quantized on the *primed* Cartesian axes defined by Eq. (1), and centered on a lattice of sites of the  $j$ th sort ( $j=1, 2$  are S sites;  $j=3, 4$  are Zn sites: see Table I). In Table VIa, VIb we give matrix components for  $s$  and  $p$  functions taking account only of first neighbor interactions for zinblende and wurtzite structures, in terms of the  $E$  integrals.<sup>3</sup> (We also worked

TABLE VI. Matrix components of energy for zinblende and wurtzite.

a. Zinblende. <sup>a</sup> $\tau_0 = (0, 0, 3/4)$ in units of $(\alpha, \beta, \gamma)$ —Eq. (2). ( $\xi, \eta, \zeta$ ) are defined in Eq. (3) of text.
$(s/s)_{13} = E_{ss}(\tau_0) \{ e^{3i\zeta/4} + e^{-i\zeta/4} [ (2 \cos \xi \cos(\eta/3) + \cos(2\eta/3)) + i(2 \cos \xi \sin(\eta/3) - \sin(2\eta/3)) ] \},$
$(s/z)_{13} = E_{sz}(\tau_0) \{ e^{3i\zeta/4} - \frac{1}{3} e^{-i\zeta/4} [ \dots ] \},$
$(s/x)_{13} = [ 4i/(6)^{1/2} ] E_{sz}(\tau_0) \sin \xi e^{i(\eta/3 - \zeta/4)},$
$(s/y)_{13} = - (2\sqrt{2}/3) E_{sz}(\tau_0) [ e^{-i(2\eta/3 + \zeta/4)} - \cos \xi e^{i(\eta/3 - \zeta/4)} ],$
$(z/z)_{13} = E_{zz}(\tau_0) e^{3i\zeta/4} + (1/9) [ 8E_{zx}(\tau_0) + E_{zz}(\tau_0) ] e^{-i\zeta/4} [ \dots ],$
$(x/x)_{13} = E_{xx}(\tau_0) [ e^{3i\zeta/4} + e^{-i(2\eta/3 + \zeta/4)} + \frac{1}{2} \cos \xi [ (4/3) E_{xx}(\tau_0) + (8/3) E_{zz}(\tau_0) ] e^{i(\eta/3 - \zeta/4)},$
$(y/y)_{13} = E_{xx}(\tau_0) [ e^{3i\zeta/4} + \frac{2}{3} \cos \xi e^{i(\eta/3 - \zeta/4)} + (1/9) [ E_{xx}(\tau_0) + 8E_{zz}(\tau_0) ] \{ e^{-i(2\eta/3 + \eta/4)} + \frac{1}{2} \cos \xi e^{i(\eta/3 - \zeta/4)} \},$
$(x/y)_{13} = (4\sqrt{3}i/9) [ E_{zz}(\tau_0) - E_{xx}(\tau_0) ] \sin \xi e^{i(\eta/3 - \eta/4)}$
$(x/z)_{13} = (4\sqrt{3}i/9\sqrt{2}) [ E_{xx}(\tau_0) - E_{zz}(\tau_0) ] \sin \xi e^{i(\eta/3 - \eta/4)}$
$(y/z)_{13} = (4/9\sqrt{2}) [ E_{xx}(\tau_0) - E_{zz}(\tau_0) ] \{ e^{-i(2\eta/3 + \zeta/4)} - \cos \xi e^{i(\eta/3 - \zeta/4)} \}.$
b. Wurtzite. <sup>b</sup> $\tau_0 = (0, 0, 3/4)$ ; $\tau_1 = (0, -2/3, -1/4)$ in units of $(\alpha, \beta, \gamma)$ —Eq. (2). ( $\xi, \eta, \zeta$ ) are defined in Eq. (3) of text.
$(n/m)_{13} = (n/m)_{24} = E_{nm}(\tau_0) e^{3i\zeta/4}$
$(n/m)_{14} = E_{nm}(\tau_1) [ (2 \cos \xi \cos(\eta/3) + \cos(2\eta/3)) + i(2 \cos \xi \sin(\eta/3) - \sin(2\eta/3)) ] e^{-i\zeta/4},$
$(n/m)_{23} = E_{nm}(\tau_1) [ (2 \cos \xi \cos(\eta/3) + \cos(2\eta/3)) - i(2 \cos \xi \sin(\eta/3) - \sin(2\eta/3)) ] e^{-i\zeta/4},$
$(n/x)_{14} = i\sqrt{3} E_{ny}(\tau_1) \sin \xi e^{i(\eta/3 - \zeta/4)},$
$(n/x)_{23} = -i\sqrt{3} E_{ny}(\tau_1) \sin \xi e^{-i(\eta/3 + \zeta/4)},$
$(n/y)_{14} = E_{ny}(\tau_1) [ e^{-i(2\eta/3 + \zeta/4)} - \cos \xi e^{i(\eta/3 - \zeta/4)} ],$
$(n/y)_{23} = -E_{ny}(\tau_1) [ e^{i(2\eta/3 - \zeta/4)} - \cos \xi e^{-i(\eta/3 + \zeta/4)} ],$
$(p/p)_{13} = (p/p)_{24} = E_{xx}(\tau_0) e^{3i\zeta/4}$
$(p/p)_{14} = E_{xx}(\tau_1) e^{-i(2\eta/3 + \zeta/4)} + 2 \cos \xi E_{xx}(\tau_1) e^{i(\eta/3 - \zeta/4)},$
$(p/p)_{23} = E_{xx}(\tau_1) e^{i(2\eta/3 - \zeta/4)} + 2 \cos \xi E_{xx}(\tau_1) e^{-i(\eta/3 + \zeta/4)},$
$(n/p)_{13} = (n/p)_{24} = (p/q)_{13} = (p/q)_{24} = (p/q)_{14} = (p/q)_{23} = 0.$

<sup>a</sup> The [  $\dots$  ] in the expressions for  $(s/z)_{13}$  and  $(z/z)_{13}$  for zinblende is the same function of  $(\xi, \eta, \zeta)$  as given inside the square brackets in the expression for  $(s/s)_{13}$ .

<sup>b</sup>  $n, m$  can be  $(s$  and  $z)$ ;  $p, q$  can be  $(x$  and  $y)$ .  $n$  and  $m$  may be equal;  $p \neq q$ .

J. Chem. Phys. **30**, 379 (1959); M. L. Glasser, J. Phys. Chem. Solids (in press); R. Parmenter (unpublished notes); F. W. Quille, Jr. Quarterly Progress Reports, Solid State and Molecular Theory Group, Massachusetts Institute of Technology, Cambridge, Mass. July 15, 1958 (unpublished) p. 28; R. C. Casella, Phys. Rev. **114**, 1514 (1959); J. L. Birman, Phys. Rev. **114**, 1490 (1959). I am indebted to Dr. Glasser, Dr. Parmenter, and Dr. Casella for making preprints of their papers available.

TABLE VII. Two-center integrals and perturbation parameters.

Zinblende
$E_{ss}(\tau_0) = E_{ss}(-\tau_0) = ss\sigma(\tau_0),$
$E_{sz}(\tau_0) = -E_{zs}(\tau_0) = sp\sigma(\tau_0),$
$E_{xx}(\tau_0) = E_{xx}(-\tau_0) = pp\sigma(\tau_0),$
$E_{zz}(\tau_0) = E_{zz}(-\tau_0) = pp\sigma(\tau_0).$
Wurtzite
$E_{ss}(\tau_0) = ss\sigma(\tau_0), \quad E_{sz}(\tau_0) = sp\sigma(\tau_0),$
$E_{ss}(\tau_1) = ss\sigma(\tau_1), \quad E_{sz}(\tau_1) = -\frac{1}{3} sp\sigma(\tau_1),$
$E_{zs}(\tau_0) = -E_{sz}(\tau_0) = -sp\sigma(\tau_0),$
$E_{zs}(\tau_1) = -E_{sz}(\tau_1) = \frac{1}{3} sp\sigma(\tau_1),$
$E_{sy}(\tau_1) = -E_{ys}(\tau_1) = -\frac{2}{3}\sqrt{2} sp\sigma(\tau_1),$
$E_{xx}(\tau_0) = E_{xx}(-\tau_0) = pp\pi(\tau_0),$
$E_{xx}(\tau_1) = E_{xx}(-\tau_1) = pp\pi(\tau_1),$
$E_{zz}(\tau_0) = E_{zz}(-\tau_0) = pp\sigma(\tau_0),$
$E_{zz}(\tau_1) = (1/9) pp\sigma(\tau_1) + (8/9) pp\pi(\tau_1) = pp\pi(\tau_1)^a$
$E_{yz}(\tau_1) = (2\sqrt{2}/9) [ pp\sigma(\tau_1) - pp\pi(\tau_1) ] = 0^a$
Perturbation Parameters
$ss\sigma(\tau_0; \text{ZB}) = ss\sigma(\tau_0; \text{Wur}),$
$sp\sigma(\tau_0; \text{ZB}) = sp\sigma(\tau_0; \text{Wur}),$
$pp\sigma(\tau_0; \text{ZB}) = pp\sigma(\tau_0; \text{Wur}),$
$ss\sigma(\tau_1; \text{Wur}) \equiv ss\sigma(\tau_0; \text{ZB}) + \delta_1,$
$sp\sigma(\tau_1; \text{Wur}) \equiv sp\sigma(\tau_0; \text{ZB}) + \delta_2,$
$pp\sigma(\tau_1; \text{Wur}) = pp\pi(\tau_1; \text{Wur})^a$
$\equiv pp\sigma(\tau_0; \text{ZB}) + \delta_3,$
$\equiv pp\pi(\tau_0; \text{ZB}) + \delta_4.$

<sup>a</sup> These equalities follow from the fact that  $E_{zx}(\tau_1; \text{Wur}) = E_{yz}(\tau_1; \text{Wur})$ , i.e., the apparent  $C_{6v}$  symmetry of the  $E_{mn}$  integrals in Wur.

out the results including second neighbor interactions but these would only unnecessarily complicate, without really clarifying, the relationships of interest. Of course, an accurate LCAO numerical calculation or interpolation should include these and any other necessary shells of neighbors.) Reduction of the  $E$  integrals to the independent ones shown, has been carried out by using the elements of crystal symmetry (Table III). It is of interest to note that although the site symmetry in wurtzite is only  $C_{3v} = 3m$  the  $E$  integrals have the higher symmetry characteristic of point group  $C_{6v} = 6m$ . This is due to the "rotational" part of the crystal symmetry operations  $6_2$  and  $m_3$ . In Table VII is given the reduction of the  $E$  integrals to two center integrals and also the definition of the four perturbation elements  $\delta_i$ , which are the matrix elements of the perturbation  $V'$  of equation (4), in terms of which we shall obtain the relationship between certain zinblende and wurtzite energy states.

Consider states along  $\Gamma - \Lambda(\text{ZB})$  and  $\Gamma - \Gamma'(\text{Wur})$ . Using the information in Tables IV and VII, we have set up the secular determinants for energies of states at the end points<sup>15</sup> ( $\Gamma$  and  $\Lambda$  and  $\Gamma'$ ), and these are

<sup>15</sup> If the wurtzite *reduced* zone is used,  $\Gamma(\text{Wur}) \equiv \Gamma'(\text{Wur})$ , and the states  $\Gamma_1'(\text{Wur})$  and  $\Gamma_6'(\text{Wur})$  are respectively  $\Gamma_3$  and  $\Gamma_6$  (see Dresselhaus, reference 14).

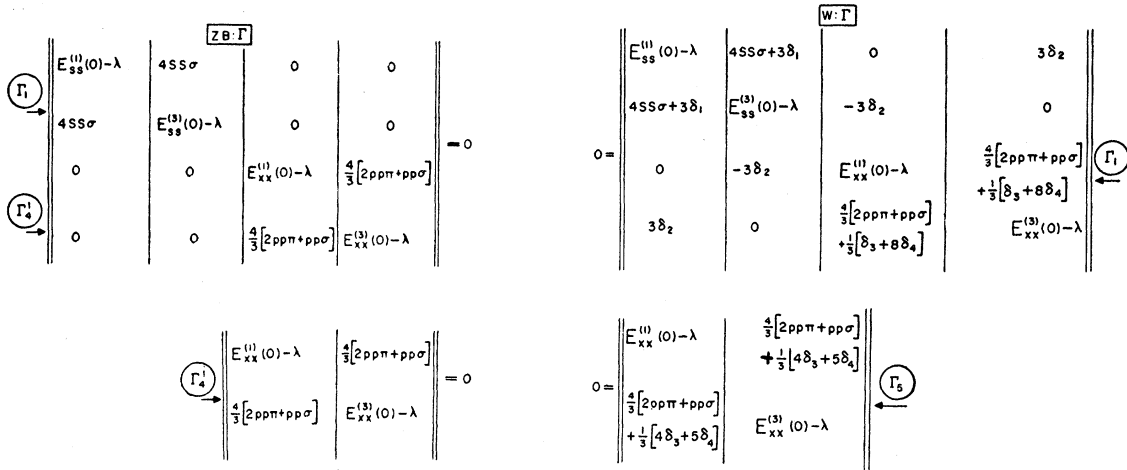


FIG. 9. Secular determinants  $\mathbf{k}=(0,0,0)$  zincblende and wurtzite. Two center, nearest neighbor approximation. For definition of the matrix elements see Tables VI and VII. Note that when all  $\delta_i \rightarrow 0$  [ $V'$  in Eq. (3)],  $\Gamma_1(\text{Wur})=\Gamma_1(\text{ZB})+\Gamma_4'(\text{ZB})$ ,  $\Gamma_5(\text{Wur})=\Gamma_4'(\text{ZB})$ .

shown in Figs. 9 and 11 in terms of the two center integrals and the  $\delta_i$  defined in Table VIII. In Figs. 10 and 12 we indicate reasonable separations of the various states in zincblende and wurtzite, assuming these occur in normal order (as seems to be the case in ZnS, according to our most recent numerical results at these points). Note the effect of the perturbation  $V'$  in mixing and shifting zincblende states to yield the corresponding wurtzite states. Since the relative change in magnitude of the corresponding matrix elements is greater at  $\Gamma$  than at  $\Lambda, \Gamma'$ , we conclude that the shift of corresponding states is greater at  $\Gamma$  than at the end points. Further, since within this simplified LCAO theory (first neighbor, 2 center) the change in matrix elements varies continuously from  $\mathbf{k}=\Gamma$  to  $\Lambda, \Gamma'$  we conclude that the shift of corresponding states varies continuously as illustrated

in Fig. 13. Now this is certainly an oversimplification, since one would hardly expect the simple  $\epsilon(\mathbf{k})$  curves shown to apply to a real material. However, in the absence of exact information, this approach enables certain conclusions to be drawn with varying degrees of accuracy. Hence, for  $\Gamma-\Lambda, \Gamma-\Gamma'$  propagation:

1. States (as well as  $\mathbf{k}$  vectors) show a correspondence along this direction.

2. The perturbation (shift and splitting)<sup>16</sup> of corresponding states depends on  $\mathbf{k}$ . For simple model (normal order of states, band extrema at  $\Gamma$ ), it appears that the perturbation is greatest at  $\Gamma$ , diminishing as  $\mathbf{k}$  approaches the zone edge. It must be pointed out that  $G(\mathbf{k})$  in wurtzite= $6\frac{1}{2}m\frac{1}{3}$  for  $\mathbf{k}$  along  $\Gamma-\Gamma'$  (Wur),  $G(\Gamma(\text{ZB}))=43m$ , and  $G(\mathbf{k})=3m$  in zincblende for other points along  $\Gamma-\Lambda$ . Hence in our approximation,  $G(\Gamma(\text{Wur}))$  is effectively a subgroup of  $G(\Gamma(\text{ZB}))$ , while along  $\Gamma-\Gamma'$  (Wur) and  $\Gamma-\Lambda(\text{ZB})$ ,  $G(\mathbf{k}(\text{Wur}))$  and  $G(\mathbf{k}(\text{ZB}))$  are effectively isomorphic.

3. At fixed  $\mathbf{k}$  the perturbation is the greater, the larger is  $V'$ . The factors influencing  $V'$  are the change in bond type (ion charge) in going from zincblende to wurtzite, as well as the departure from ideality of the wurtzite structure. Another factor affecting  $V'$  will be mentioned in discussing faulted structures: the probability of faulting,  $\alpha$ .

4. As  $\delta_i \rightarrow 0$  (wurtzite  $\rightarrow$  zincblende):

$$\left. \begin{aligned} \Gamma_1(\text{Wur}) &= \Gamma_1(\text{ZB}) + \Gamma_4'(\text{ZB}) \\ \Gamma_5(\text{Wur}) &= \Gamma_4'(\text{ZB}) \end{aligned} \right\} \text{ at } \mathbf{k}=(000),$$

$$\left. \begin{aligned} \Gamma_1(\text{Wur}) &= \Lambda_1(\text{ZB}) \\ \Gamma_5(\text{Wur}) &= \Lambda_3(\text{ZB}) \end{aligned} \right\} \text{ and } \Gamma-\Gamma'(\text{Wur}).$$

For  $\Gamma-M$  and  $\Gamma-K$  propagation the situation is more complicated. First, it is not clear how to compare

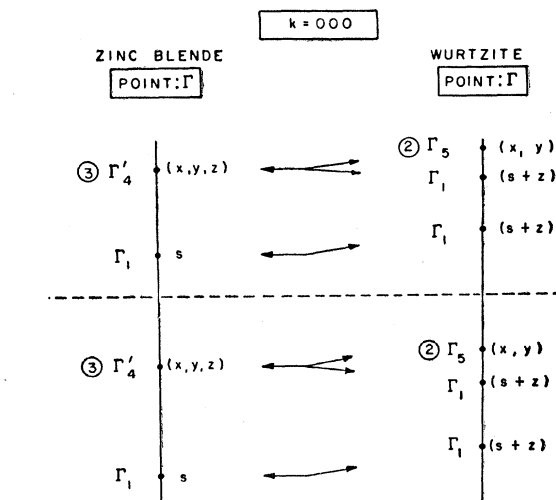


FIG. 10. States at  $\mathbf{k}=(0,0,0)$ , illustrating shift and splitting of corresponding states. States are shown in "normal" order and separated by roughly the amounts indicated in the ZnS calculation now in progress.

<sup>16</sup> See, e.g., E. P. Wigner, *Gruppen-theorie* (Edwards Brothers, Ann Arbor, Michigan, 1944), p. 128.

$$\begin{array}{c}
 \text{ZB: } \Lambda \\
 \left( \Lambda \right) \begin{vmatrix} E_{ss}^{(1)}(0) - \lambda & 2\gamma(ss\sigma) & 0 & -2\gamma S p \sigma \\ 2\gamma^* (ss\sigma) & E_{ss}^{(3)}(0) - \lambda & 2\gamma^* S p \sigma & 0 \\ 0 & 2\gamma S p \sigma & E_{xx}^{(1)}(0) - \lambda & 2\gamma [4pp\pi - pp\sigma]/\delta \\ -2\gamma^* S p \sigma & 0 & 2\gamma [4pp\pi - pp\sigma]/3 & E_{xx}^{(3)}(0) - \lambda \end{vmatrix} = 0 \\
 \\
 \left( \Lambda_3 \right) \begin{vmatrix} E_{xx}^{(1)}(0) - \lambda & \frac{2}{3} [pp\pi + 2pp\sigma] \gamma \\ \frac{2}{3} [pp\pi + 2pp\sigma] \gamma^* & E_{xx}^{(3)}(0) - \lambda \end{vmatrix} = 0 \\
 \gamma = e^{-\pi i/4}
 \end{array}
 \qquad
 \begin{array}{c}
 \text{W: } \Gamma' \\
 0 = \begin{vmatrix} E_{ss}^{(1)}(0) - \lambda & (ss\sigma + 3\delta_1)\gamma & 0 & -(2Sp\sigma + \delta_2)\gamma \\ (2SS\sigma + 3\delta_1)\gamma^* & E_{ss}^{(3)}(0) - \lambda & (2Sp\sigma + \delta_2)\gamma^* & 0 \\ 0 & (2Sp\sigma + \delta_2)\gamma & E_{xx}^{(1)}(0) - \lambda & \frac{2}{3}\gamma [4pp\pi - pp\sigma] \\ -(2Sp\sigma + \delta_2)\gamma^* & 0 & \frac{2}{3}\gamma^* [4pp\pi - pp\sigma] & E_{xx}^{(3)}(0) - \lambda \end{vmatrix} \left( \Gamma'_1 \right) \\
 \\
 0 = \begin{vmatrix} E_{xx}^{(1)}(0) - \lambda & \frac{2}{3}\gamma [pp\pi + 2pp\sigma] \\ \frac{1}{2}\gamma^* [pp\pi + 2pp\sigma + \frac{1}{2}(5\delta_4 + 4\delta_3)] & E_{xx}^{(3)}(0) - \lambda \end{vmatrix} \left( \Gamma'_5 \right)
 \end{array}$$

FIG. 11. Secular determinants: at  $\mathbf{k}=\Lambda$ ,  $\mathbf{k}=\Gamma'$  for zincblende and wurtzite, respectively. Note that as  $\delta_i \rightarrow 0$ ;  $\Gamma'_1(\text{Wur}) = \Lambda_1(\text{ZB})$ ,  $\Gamma'_5(\text{Wur}) = \Lambda_3(\text{ZB})$ .

$\mathbf{k}$  vectors: three choices have been mentioned above. In addition the  $G(\mathbf{k})$  of zincblende and wurtzite along these directions are not simply related. For example  $G(\mathbf{k})$  for  $\Gamma-K(\text{ZB})$  is  $C_{1h}$  (see Table III) where  $m'$  is a mirror plane containing  $\Gamma-K(\text{ZB})$  but at an angle to the  $x'y'$  zone section of Fig. 5, while the  $G(\mathbf{k})$  for  $\Gamma-K(\text{Wur})$ , except at  $K$ , is isomorphic to  $C_{1h}$  but the "mirror" plane is the glide plane  $m_3$ . In addition, at  $K$  wurtzite the  $G(\mathbf{k})$  is isomorphic to  $C_{3v} = 3m$  (see Tables III and V). This comes about because the points in Fig. 5 labelled  $K, K', K''$  are equivalent (differ by a lattice vector in the Fourier space for wurtzite). This is not true for the corresponding zincblende points, since the lattice vectors in the zincblende Fourier space are not in the plane of Fig. 5 nor does any combination of such vectors send  $K(\text{ZB})$  into a vector rotated by  $2\pi/3$ . Consequently at  $K(\text{Wur})$  there is a degeneracy: representation  $K_3(\text{Wur})$  is double degenerate. In Fig. 14 secular determinants at  $K(\text{Wur}) = \mathbf{k}(\text{ZB}) = (\pi/3, \pi, 0)$  are shown and in Fig. 15 states are listed in a "normal" order. Consequently, a simple perturbation argument does not hold in this direction, for zincblende-wurtzite states. Evidently the same conclusion holds for zincblende-wurtzite states along  $\Gamma-M$ .

6. BAND STRUCTURE OF A MIXED CRYSTAL; EFFECT OF FAULTING

The correspondences established above can help us understand the band structure of mixed and faulted crystals after we have established some geometric-crystallographic preliminaries.

Actual synthetic crystals of ZnS,<sup>17</sup> SiC, and related materials often show structural imperfections: stacking faults (random and periodic) and twinning. In fact structurally homogenous ZnS (either zincblende or wurtzite pure structure) is an extreme rarity in our ex-

perience. A typical single crystal needle of ZnS is shown in Fig. 16. This crystal was grown in this laboratory by H. Samelson, and shows (x-ray and optical) features characteristic of  $[111]$  faulting and twinning. In terms of the stacking diagram, Fig. 17(a), 17(b) shows a mixed crystal (wurtzite twinned on zincblende) and a particular kind of stacking fault: the rotation twin in zincblende. The latter kind of fault is helpful in understanding what we shall call the "polar effect" in producing a barrier.

(a) *Polar effect*.—Consider a crystal consisting of many regions of zincblende rotation-twinned with respect to each other. The polar axis (unique "c") has the same direction throughout the crystal. At each twin plane however, the local stacking is characteristic of 3 layers of wurtzite structure [i.e.,  $\dots BCB \dots$  in Fig. 17(a)]. The atoms in the twin plane region are subject

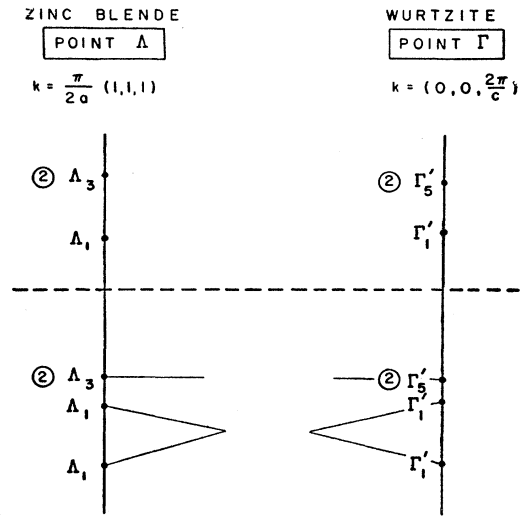


FIG. 12. States at  $\mathbf{k}=\Lambda$  and  $\Gamma'$ , in "normal" order and separated as indicated in the ZnS calculation now in progress.

<sup>17</sup> H. Müller, Neues Jahr. Mineral. Abhandl. 84, 1, 43 (1952); L. W. Strock and V. Brophy, Am. Mineralogist 40, 94 (1955).

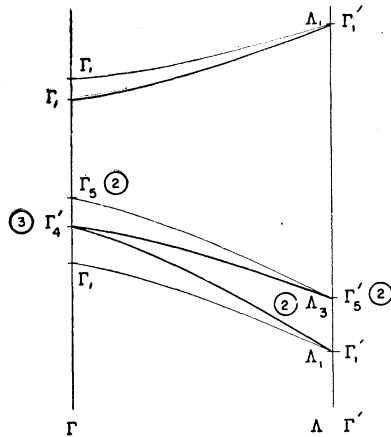


FIG. 13. Shift of corresponding states along  $\Gamma-\Lambda$  (ZB) and  $\Gamma-\Gamma'$  (Wur) (schematic). Heavy line is for zincblende, light one for wurtzite. This illustrates (in simple if exaggerated fashion) the conclusion that the shift of corresponding states is  $\mathbf{k}$  dependent, and apparently greater at the origin than at the end of the zones, for the simplified model treated. The states  $\Gamma_4'$  (ZB) (upper valence state) and  $\Gamma_1$  (ZB) (lower conduction state) and corresponding wurtzite states are illustrated. For Wur' (faulted wurtzite-like structure) separations at each  $\mathbf{k}$  depend upon  $\alpha$ , the probability of faulting.

to unbalanced forces causing departure from normal positions. The local (uniaxial) strain gives rise to a sheet of polarized material<sup>18</sup> (piezoelectric plus pyroelectric effects) included in the zincblende. This thin sheet of a dipole layer is equivalent to a charge double layer, and it is well known that the potential exhibits a discontinuity on passing from one to another side of such a charge double layer.<sup>19</sup> The discontinuity of potential is a barrier (see Fig. 18). We call this a polar effect since the locked-in strain and polarization arises largely because of the polar (partial ionic) character of the chemical bond in this material. Quantitative work

on the magnitude of locked-in strain and potential discontinuity still remains to be done.

(b) *Symmetry effect.*—Consider the mixed crystal in Fig. 17 (b) and let us ignore distortions and polarizations in the boundary layer, and assume unchanged  $[111]$  interplanar spacings in the twinned crystal. Hence our mixed crystal consists of ideal zincblende-wurtzite regions in series for propagation parallel to  $[111]$ , and in parallel (for propagation perpendicular to  $[111]$ ). Because of the identity of corresponding zincblende and wurtzite  $\mathbf{k}$  vectors along  $\Gamma-\Lambda$  and  $\Gamma-\Gamma'$ , respectively, we see that a plane wave propagating parallel to  $[111]$  can pass undistorted from zincblende to wurtzite sides of the boundary for all  $\mathbf{k}$  parallel to  $[111]$ . Otherwise stated we may preserve  $\mathbf{k}$  on either side of the boundary. Now assume that in the zincblende region the crystal potential is  $V$  (ZB), and in wurtzite it is  $V$  (Wur). Then we may use Fig. 13 to determine relative location of energy levels of the appropriate states on either side of the boundary. For example, at  $\mathbf{k} = (0, 0, 0)$  zincblende states are shifted and split to yield corresponding wurtzite states as shown in Fig. 9. The result is indicated in Fig. 19, where the existence of a barrier (energy discontinuity in both valence and conduction bands) is shown schematically. We emphasize that this barrier arises solely because of change in the symmetry of the crystal potential  $V(r)$  by calling this the *symmetry effect*. Further, the barrier height (discontinuity in energy at a fixed  $\mathbf{k}$ ) depends on  $\mathbf{k}$  (i.e., electron energy) and should diminish as  $\mathbf{k}$  approaches the zone edge if Fig. 12 applies. Note that one may introduce a common reference level of potential and also that the vertical separation of the bands at fixed  $\mathbf{k}$ , labelled  $\Delta E_{ZB}$  and  $\Delta E_W$ , is characteristic of each of the structurally pure zincblende or wurtzite regions. Hence a given mixed crystal will show optical evidence of the simultaneous existence of both band gaps. The wavelength dependence of the

$$\begin{aligned}
 & \text{[ZB]: } \mathbf{k} = (\frac{\pi}{3}, \pi, 0) \\
 & \begin{vmatrix} E_{ss}^{(1)}(0) - \lambda & Ss\sigma & 0 & \sqrt{3}Sp\sigma & 0 & Sp\sigma(\frac{\sqrt{2}}{2} + \sqrt{2}) \\ Ss\sigma & E_{ss}^{(3)}(0) - \lambda & -\sqrt{3}Sp\sigma & 0 & -Sp\sigma(\frac{\sqrt{2}}{2} + \sqrt{2}) & 0 \\ 0 & \sqrt{3}Sp\sigma & E_{xx}^{(1)}(0) - \lambda & \frac{1}{3}(pp\sigma - pp\pi) & 0 & \frac{1}{\sqrt{6}}(pp\sigma - pp\pi) \\ -\sqrt{3}Sp\sigma & 0 & \frac{1}{3}(pp\sigma - pp\pi) & E_{xx}^{(3)}(0) - \lambda & -\frac{1}{\sqrt{6}}(pp\sigma - pp\pi) & 0 \\ 0 & Sp\sigma(\frac{\sqrt{2}}{2} - \frac{1}{2}) & 0 & \frac{1}{\sqrt{6}}(pp\sigma - pp\pi) & E_{xx}^{(1)}(0) - \lambda & \frac{2}{3}(4pp\pi - pp\sigma) \\ Sp\sigma(\frac{\sqrt{2}}{2} - \frac{1}{2}) & 0 & -\frac{1}{\sqrt{6}}(pp\sigma - pp\pi) & 0 & \frac{2}{3}(4pp\pi - pp\sigma) & E_{xx}^{(3)}(0) - \lambda \end{vmatrix} = 0 \\
 & \begin{vmatrix} E_{xx}^{(1)}(0) - \lambda & pp\pi(\frac{1}{3} - \frac{2}{3}\sqrt{3}) \\ pp\pi(\frac{1}{3} + \frac{2}{3}\sqrt{3}) & E_{xx}^{(3)}(0) - \lambda \end{vmatrix} = 0 \\
 & \text{[W]: } \mathbf{k} = (\frac{\pi}{3}, \pi, 0) + \mathbf{K} \\
 & \begin{vmatrix} E_{ss}^{(1)}(0) - \lambda & Ss\sigma & 0 & Sp\sigma \\ Ss\sigma & E_{ss}^{(3)}(0) - \lambda & -Sp\sigma & 0 \\ 0 & -Sp\sigma & E_{xx}^{(1)}(0) - \lambda & pp\sigma \\ Sp\sigma & 0 & pp\sigma & E_{xx}^{(3)}(0) - \lambda \end{vmatrix} \leftarrow \text{K}_1 \\
 & \begin{vmatrix} E_{xx}^{(1)}(0) - \lambda & pp\pi \\ pp\pi & E_{xx}^{(3)}(0) - \lambda \end{vmatrix} \leftarrow \text{K}_2
 \end{aligned}$$

FIG. 14. Secular determinants at  $K$  (Wur) =  $(\pi/3, \pi, 0) = k$  (ZB).

<sup>18</sup> J. F. Nye, *Physical Properties of Crystals* (Oxford University Press, Oxford, 1957), appendix E<sub>1</sub>. J. Birman, *Domains of Polarization and Anomalous Birefringence in Twinned Zincblende* (Sylvania report, 1957, unpublished).  
<sup>19</sup> J. A. Stratton, *Electromagnetic Theory* (McGraw-Hill Book Company, New York, 1941), p. 189.

anomalous photovoltage in twinned and faulted crystals of ZnS is probably related to this property.<sup>20</sup> The existence of barriers for conduction parallel to  $[111]$  has already been noted experimentally for faulted ZnS single crystals, and in fact there seems to be some evidence of more ohmic behavior at higher field strengths (higher electron energy and therefore  $\mathbf{k}$  near the zone edge) which would corroborate the model of lower barrier height at larger  $\mathbf{k}$ .<sup>21</sup>

Of course the actual barriers exist because of both *polar* and *symmetry* effects and much more work needs to be done before these are unscrambled. Conduction perpendicular to “ $c$ ” involves carrier transport in zincblende regions, wurtzite regions, and within the barrier region. Quantitative analysis of conduction in this direction would involve averages over the  $\Gamma-M$ ,  $\Gamma-K$  directions in both zincblende and wurtzite, and lacking precise experimental or theoretical information on band structures would be premature at this time.

(c) *Randomly faulted structure: Wur’.*—Consider a region of a crystal which in terms of the stacking diagram is neither 2 layer nor 3 layer but rather where the stacking shows one dimensional stacking disorder. That is, we may characterize the structure by the probability of faulting  $\alpha$ .<sup>17</sup> The local potential in such a region of random faulting will fluctuate but it seems reasonable to relate it to the pure zincblende and wurtzite structures’ potential on the average by

$$V(\text{ZB}) = V(\text{Wur}') + V'(\alpha) = V(\text{Wur}) + V', \quad (5)$$

where  $\text{Wur}'$  means the randomly faulted, wurtzite-like structure, and the perturbation  $V'(\alpha)$  depends upon  $\alpha$ . The exact nature of this dependence is of great importance, but is a problem beyond the scope of this

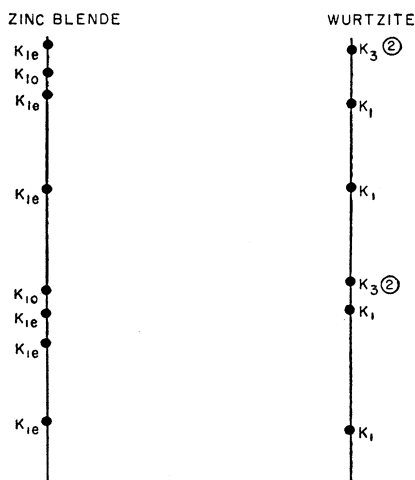


FIG. 15. States at  $K(\text{Wur}) = \frac{1}{2}(\pi/3, \pi, 0)$  in a “normal” order. No “simple” correspondence between states exists here as in the cases of propagation along  $\Gamma-A$ ;  $\Gamma-\Gamma'$ .

<sup>20</sup> G. Cheroff and S. P. Keller, Phys. Rev. **111**, 98 (1958); A. Lempicki, Phys. Rev. **113**, 1204 (1959).

<sup>21</sup> Lempicki, Frankl, and Brophy, Phys. Rev. **107**, 1238 (1957).

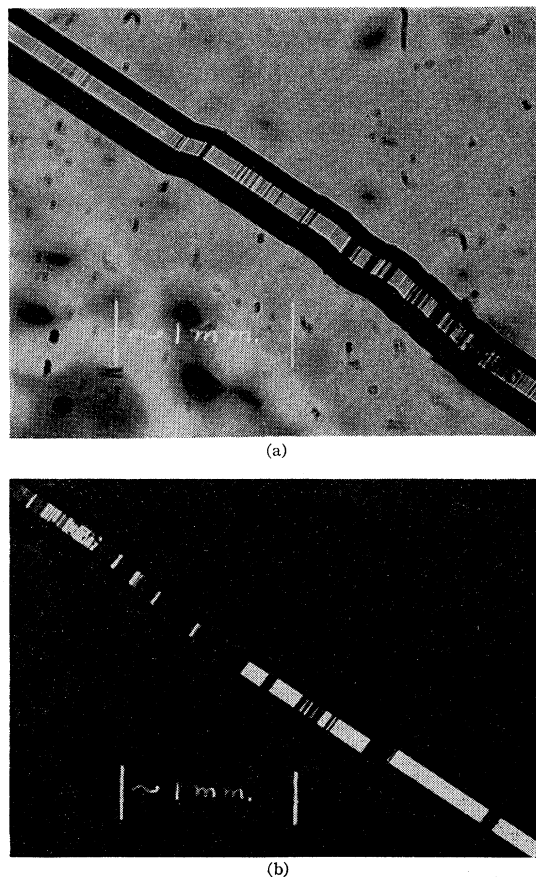


FIG. 16. Photomicrographs of a synthetic ZnS crystal needle. Upper: using unpolarized white light; lower: under crossed Nicols using convergent plane polarized white light (the crystal has been rotated about its  $c$  axis in the lower photograph). The  $c$  axis is directed along the needle, perpendicular to the striations and in the plane of the photograph. Note the alternation of optically isotropic bands (zincblende) and birefringent bands (pure wurtzite, or faulted wurtzite:  $\text{Wur}'(\alpha)$ , regions). Photograph courtesy of H. Samelson and L. Ankerson.

paper. For example, we might define  $\alpha$  so that  $\alpha=0$  (perfect structure) means wurtzite structure and then  $V'(\alpha=0) = V'$ , while  $\alpha=1$  means zincblende structure so that  $V'(\alpha=1) = 0$ . If (5) holds and we assume that we can always choose a  $\mathbf{k}$  parallel to the “ $c$ ” axis, ranging from  $\mathbf{k} = (0, 0, 0)$  to  $\mathbf{k} = (0, 0, \pi)$  (see Table IV) (i.e., that there is always a plane wave of wavelength  $\lambda = 2d_{111}$  which can be propagated), then we may carry out the LCAO treatment relating the  $\text{Wur}'$  structure to the zincblende as we did for the zincblende-wurtzite structures. Now, however, at any  $\mathbf{k}$  (parallel to “ $c$ ”) the shift and splitting of “corresponding”  $\text{Wur}'$  states will depend on  $\alpha$ . It is of interest that the correspondence between states still seems to apply for propagation parallel to “ $c$ ”. For propagation perpendicular to “ $c$ ” we may relate  $\text{Wur}'$  states to wurtzite states, by using (5). (It should be pointed out, however, that a randomly faulted  $\text{Wur}'$  structure will no longer belong to space group  $C_{6v}^4$ : the  $6_2$  and  $m_2$  operations will be lost and the

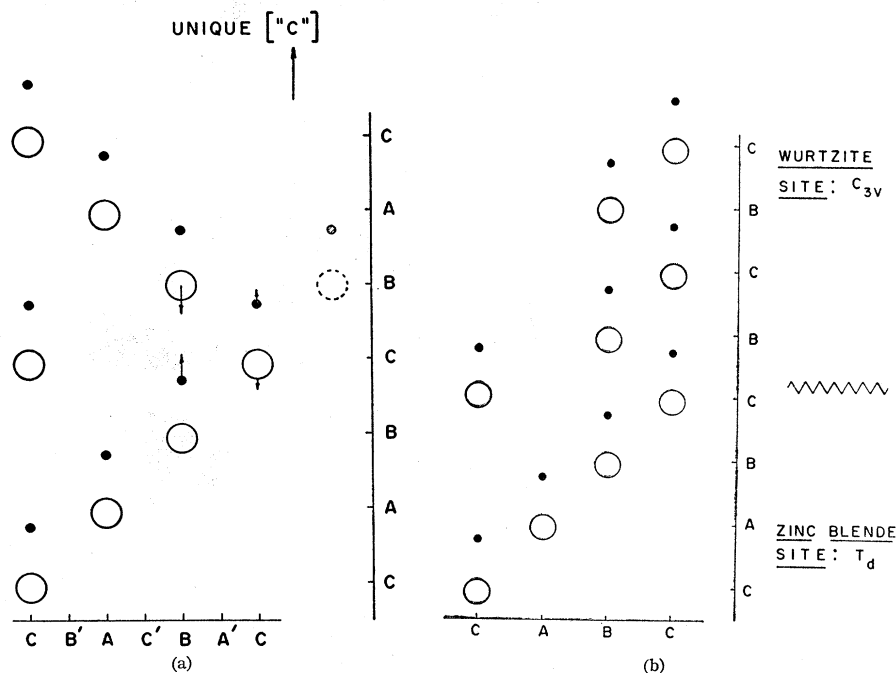


FIG. 17. (a) Stacking diagram of rotation-twinned zincblende. Compare Fig. 4. The dotted and shaded circles show stacking for the pure zincblende structure. Note the 3 layers of wurtzite structure at the rotation twin plane:  $B, C, B$  and the probable atom/ion displacements from "ideal" positions due to unbalanced forces in the twin plane (arrows). This locked in strain gives rise to a "polar" effect on the band structure for propagation  $(\mathbf{k})$  along "c." (b) zincblende-wurtzite mixed crystal. Regions of zincblende may alternate with regions of wurtzite in a real crystal and within each region the potential may show *substantially* the zincblende or wurtzite site symmetry, as illustrated by optical properties shown in Fig. 16.

site symmetry at  $A, B, C$  sites would be  $C_{3v}=3m$ . This would not affect the simplified LCAO approach as used here.)

In any event, if the definition of  $\alpha$  given above holds, it would follow that the extremes of optical band gap (vertical energy band separations at some  $\mathbf{k}$ ) should be for pure zincblende and wurtzite structures, the gap of a crystal with random faulting lying always between these extremes. Experimental work to test this hypothesis would be of considerable interest.

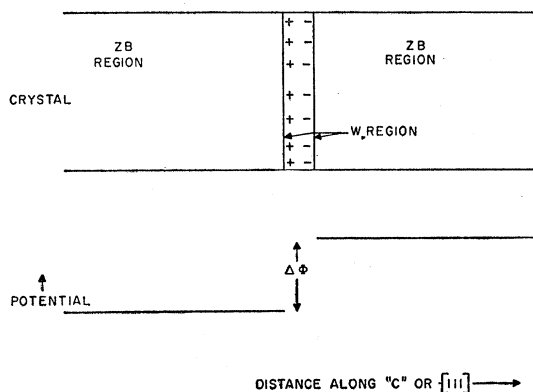


FIG. 18. Band structure: rotation-twinned zincblende illustrating the barrier caused by a "polar" effect. This is due to a thin layer of locked-in wurtzite and hence polarization (due to pyroelectric and piezoelectric effects), or an inner "double layer," at the twin plane.

## 7. CONCLUSION AND SUMMARY

The relationship between energy bands of a compound in zincblende and wurtzite structures was discussed in the simplified LCAO framework. For propagation parallel to the "c" axis ( $\Gamma-A$  or  $\Gamma-\Gamma'$ ) wurtzite states may be regarded as perturbed zincblende states. The magnitude of the perturbation  $V'$  in Eq. (4) depends on (a) difference in bond type (e.g., effective charge) in the two structures, and (b) departure of the wurtzite structure from ideality. Consequently, the amount of the perturbation of corresponding zincblende and pure wurtzite states depends on these too. Along  $\Gamma-M$  and  $\Gamma-K$  in both zincblende and wurtzite it is possible to compare  $\mathbf{k}$  vectors but the states along these lines are not simply related. This follows because there is not a simple relation between the group of the wave vector  $G(\mathbf{k})$  along this line for zincblende and wurtzite structures, as there is for propagation along "c" in the two structures, where  $G(\mathbf{k})$  for wurtzite is either a subgroup of, or isomorphic to, the corresponding  $G(\mathbf{k})$  for zincblende.

Experimental results on ZnS and SiC band gaps in zincblende and wurtzite structures<sup>22</sup> suggest that some general relationship exists between the band *gaps* (relative displacements of various conduction and valence band states) of a compound in zincblende and

<sup>22</sup> H. R. Phillip, Phys. Rev. **111**, 440 (1958); F. A. Kroeger, Physica **7**, 1 (1940).

wurtzite structures. We have in Fig. 12 a hint of such a general relationship, although Fig. 12 applies only to a simplified case within the already simplified LCAO method. In particular we would like to know: do band extremes occur at corresponding (as we have defined them) points or lines in zincblende and wurtzite? If not then what determines a shift of the extremes when going from one to another structure?

For a mixed crystal of zincblende twinned on wurtzite we find energy ( $\mathbf{k}$ ) dependent barriers for propagation parallel to the "c" axis (the same  $\mathbf{k}$  can be used on either side of the boundary plane). We identify two effects as producing these barriers: (a) a polar effect, (b) a symmetry effect. The polar effect is illustrated by rotation-twinned zincblende where the boundary (twin) layer gives rise to a locked-in double layer across which the potential is discontinuous. The symmetry effect is due to change in symmetry of the crystal potential on passing from wurtzite to zincblende regions and gives rise to the  $\mathbf{k}$  dependence of barrier height. A mixed crystal should show evidence of both zincblende and wurtzite gaps in its optical absorption; the wavelength dependence of the anomalous photovoltage may be related to this.<sup>20</sup>

For the randomly faulted wurtzite-like structure:  $Wur'(\alpha)$ , we expect a smooth progression of gap width from pure zincblende to the pure wurtzite depending on  $\alpha$  (probability of faulting) which controls  $V'(\alpha)$ , in Eq. (5). Hence assuming that all  $\mathbf{k}$  are allowed from  $\mathbf{k} = (0, 0, 0)$  to  $\mathbf{k} = (0, 0, \pi)$  ( $\Gamma'$  or  $\Lambda$ ), (see Table IV), i.e., that plane waves of wavelength as short as  $\lambda = 2d_{111}$  can be propagated parallel to "c," the effective gap at any  $\mathbf{k}$  (along "c") will depend upon  $\alpha$  in that local region. Similarly, the barrier height (symmetry effect) on transition from a zincblende region to a  $Wur'$  region will depend upon the  $\alpha$  of the latter. Propagation perpendicular to "c" in such a region will involve carrier motion on the close-packed sheets ( $[111]$  planes) within zincblende, wurtzite,  $Wur'(\alpha)$ , or barrier regions.

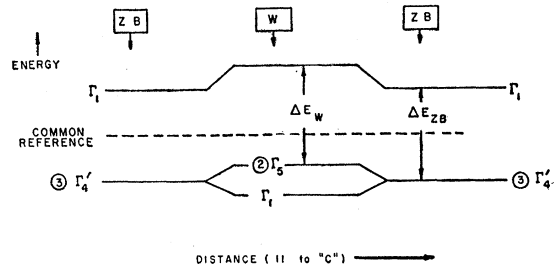


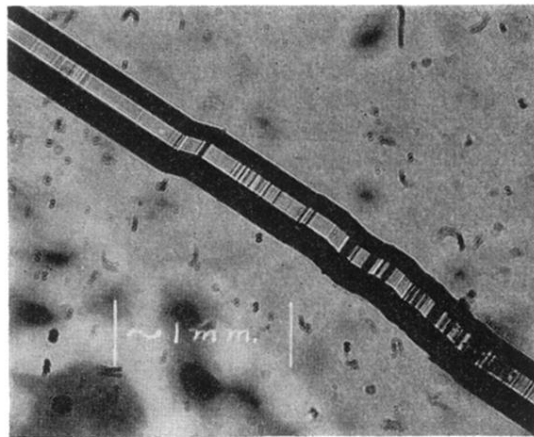
FIG. 19. Band structure of a mixed crystal illustrating the "symmetry effect" or production of a barrier due to the shift and splitting of corresponding states. The situation shown is for constant  $\mathbf{k}$  propagation on both sides of the barrier,  $\mathbf{k}$  parallel to "c." Barrier heights (discontinuities) as well as absolute magnitudes of energy separations ( $\Delta E_{ZB}$ ,  $\Delta E_W$ ) are  $\mathbf{k}$  dependent. To obtain a proper "symmetry" effect band structure at a different  $\mathbf{k}$  one uses Fig. 13 (or its correct equivalent) and draws a vertical line at the appropriate  $\mathbf{k}$ . The figure is schematic, as the magnitudes of barriers, splittings, and shifts of bands with respect to the common reference level are not known for any particular material. For example, it is entirely possible that the valence and conduction bands (for some particular material) are all shifted away from the common reference level, on passing from the zincblende to the wurtzite parts of the mixed crystal.

As a final word, the simplicity of the arguments used in this paper must be emphasized. A really self-consistent dynamical theory of electron propagation and band structure analogous to the work on x-ray and electron diffraction in faulted materials now under way,<sup>23</sup> remains for the future.

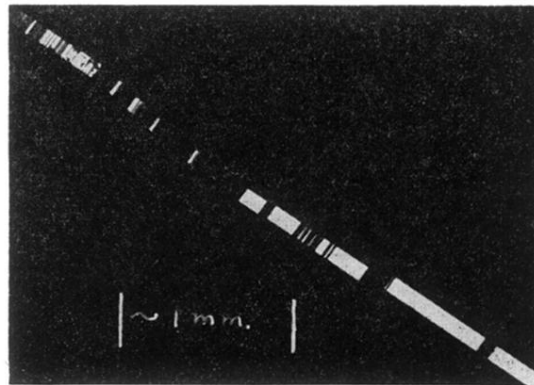
## 8. ACKNOWLEDGMENTS

It is a pleasure to acknowledge many discussions of this work with my colleagues at the Research Laboratories, in particular, the discussions with Dr. L. W. Strock and Mr. V. A. Brophy on crystallography, and with Dr. H. Samelson, Dr. G. Neumark, and Mr. A. Lempicki on various other aspects of the work.

<sup>23</sup> See M. J. Whelan and P. B. Hirsch, *Phil. Mag.* **2**, 23, 1121, 1303 (1957).



(a)



(b)

FIG. 16. Photomicrographs of a synthetic ZnS crystal needle. Upper: using unpolarized white light; lower: under crossed Nicols using convergent plane polarized white light (the crystal has been rotated about its  $c$  axis in the lower photograph). The  $c$  axis is directed along the needle, perpendicular to the striations and in the plane of the photograph. Note the alternation of optically isotropic bands (zincblende) and birefringent bands (pure wurtzite, or faulted wurtzite: Wur'( $\alpha$ ), regions). Photograph courtesy of H. Samelson and L. Ankerson.